CFD MODELING AS A TOOL FOR ASSESSING OUTDOOR THERMAL COMFORT CONDITIONS IN URBAN SETTINGS IN HOT ARID CLIMATES

Khalid Setaih, PhD Candidate
School of Architecture, Planning and Landscape, Newcastle University,NE1 7RU, UK
Email: k.m.setaih@newcastle.ac.uk ; khalid@setaih.com ; http://www.setaih.com

Neveen Hamza, PhD, Senior Lecturer
School of Architecture, Planning and Landscape, Newcastle University,NE1 7RU, UK
Email: neveen.hamza@newcastle.ac.uk

Mohammed A. Mohammed, PhD Candidate
School of Architecture, Planning and Landscape, Newcastle University,NE1 7RU, UK
Email: a.m.mohammed@newcastle.ac.uk

Steven Dudek, PhD, Lecturer
School of Architecture, Planning and Landscape, Newcastle University,NE1 7RU, UK
Email: steven.dudek@newcastle.ac.uk

Tim Townshend, PhD , Senior Lecturer
School of Architecture, Planning and Landscape, Newcastle University,NE1 7RU, UK
Email: tim.townshend@newcastle.ac.uk

SUMMARY: *Computational Fluid Dynamics (CFD) is increasingly being used as a tool for the analysis of outdoor and indoor air flow and thermal conditions. With over half of the world's population living in cities, rapid population growth and dense urban development has increasingly led to the phenomenon of urban heat islands, which in turn contribute to the deteriorating air quality and thermal discomfort in outdoor urban public spaces. In hot arid countries, changes in the characteristics of the urban microclimate are observed due to dense urbanization, high-rise buildings, and industrialization of the building processes and materials, leading to a reduction in thermal comfort in outdoor and indoor spaces. This research highlights the potential of adopting Computational Fluid Dynamics (CFD) as a simulation technique to investigate the complex fluid flow patterns in urban thermal environments, and investigates methods intended to prolong thermal comfort in public places. It discusses the advantages and limitations of CFD tools and the procedural guidelines for conducting CFD simulation. This paper also gives examples of case studies of CFD assessment for indoor and outdoor urban environments, and the practical use of RANS solver in comparison with LES, DES, and DNS models. Finally the paper highlights a case study of a CFD simulation using a RANS turbulence model of an urban street in the hot arid city of Madinah, Saudi Arabia.*

KEYWORDS: *Computational Fluid Dynamics; CFD Guideline; Outdoor Urban Environment; Thermal Comfort, Wind Comfort.*

1. INTRODUCTION

Thermal comfort is an essential factor that should be considered in an urban design process of outdoor public spaces, which can have a beneficial impact on the social and economic behavior aspects of people using these places. Comfortable urban microclimates can encourage people to use outdoor spaces for relaxation, socializing, walking and can thus increase the commercial activity. Traditional urban environments in many Middle Eastern cities have been characterized by the cooling effects created by their shaded narrow streets, thermal mass of the surrounding buildings and attention to orienting the streets towards the prevailing wind directions. Nowadays, the introduction of Western and European urban planning and massing concepts have led to dense urbanization, high-rise buildings and an industrialization of the building processes and materials (Isenstadt and Rizvi, 2008). This has also led to changes in the urban microclimate characteristics in many outdoor and indoor spaces due to the reduction of vegetation and the production of anthropogenic heat, both of which have resulted in human thermal discomfort (Fig. 1).
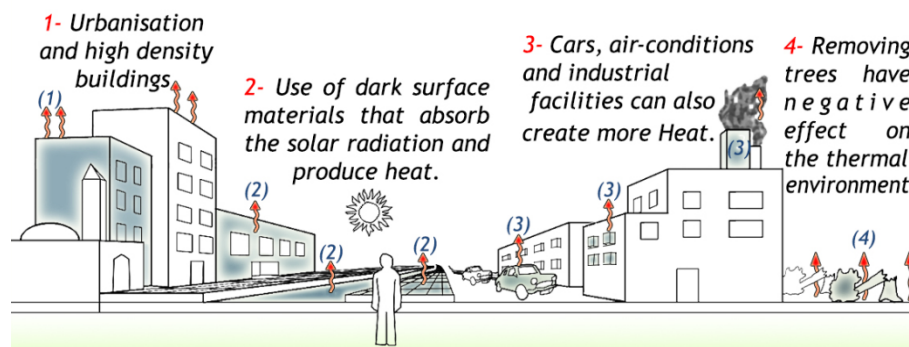

FIG. 1: Factors that can cause thermal discomfort in a city.

According to Coutts et al. (2007) compact urban areas have a large heat storage fraction due to changes in the ground surface characteristics through reduced vegetation cover and the use of low reflective materials (dark surfaces that have reduced albedo), and mostly through an increased built-up surface area (i.e. height-width ratio). This in turn has resulted in human dissatisfaction with the surrounding thermal environments, as higher ambient temperatures are found due to the urban heat island effect (Moonen et al., 2012; Setaih et al., 2013a). The study of thermal comfort in non-peak summer conditions in hot arid areas suggests a higher tolerance of the thermal conditions in outdoor spaces than in indoor spaces. A study of outdoor pedestrian thermal comfort in Madinah, Saudi Arabia, has demonstrated that the thermal comfort index value of PET (physiological equivalent temperature) in a high urban density street reached an average sensation temperature of 29°C in Autumn 2012 and 33.4^{o}C in Spring 2013, a range which lies above the indoor thermal comfort band (i.e. between 17 to 23°C) (Setaih et al., 2013b). Figure 2 shows the PET temperature where the urban heat island is observed in the city, against air temperature, mean radiant temperature (MRT) and timescale for April. The PET thermal sensation is mainly affected by the MRT (Setaih et al., 2013b). Thermal discomfort is attributed to the lack of plantation and water ponds in regions of low humidity of Saudi Arabia; the use of asphalt and concrete that have low a reflectivity to solar radiation and a high thermal storage capacity; and the fact that the orientation of buildings and streets are not planned in consideration with the prevailing wind directions and solar angles.

Therefore, in industrialized countries, people on average tend to spend most of their time indoors with about 10% of their time outdoors in summer time and only 2-4% in winter time (Hoppe, 2002; Taleb and Taleb, 2014). Murakami et al. (1999) have pointed out that the outdoor pedestrian thermal comfort can be enhanced by considering the following urban interventions in hot environments (Fig.3), which are:

- Using water features and plantation to increase latent heat loss from the ground. This process can have cooling effects due to evaporation and evapotranspiration, which is suitable for hot dry climatic condition regions;

- Using vegetation and trees for shade to reduce the amount of intensive solar radiation reaching ground surfaces;
- Considering arranging buildings along the wind direction (including the urban aspect ratio and the orientation of urban streets) to increase the air velocity around buildings and in urban open spaces at pedestrian level;
- Using surface materials as ground covers for urban spaces ground covers and building facades with a high solar radiation reflectivity (lighter colors) is also important for improving the microclimatic condition of outdoor urban spaces, and thus the thermal comfort level (Tan and Fwa, 1992). Nevertheless, light materials if not used with an appropriate urban design concept may lead to heat trapped in the spaces between buildings.
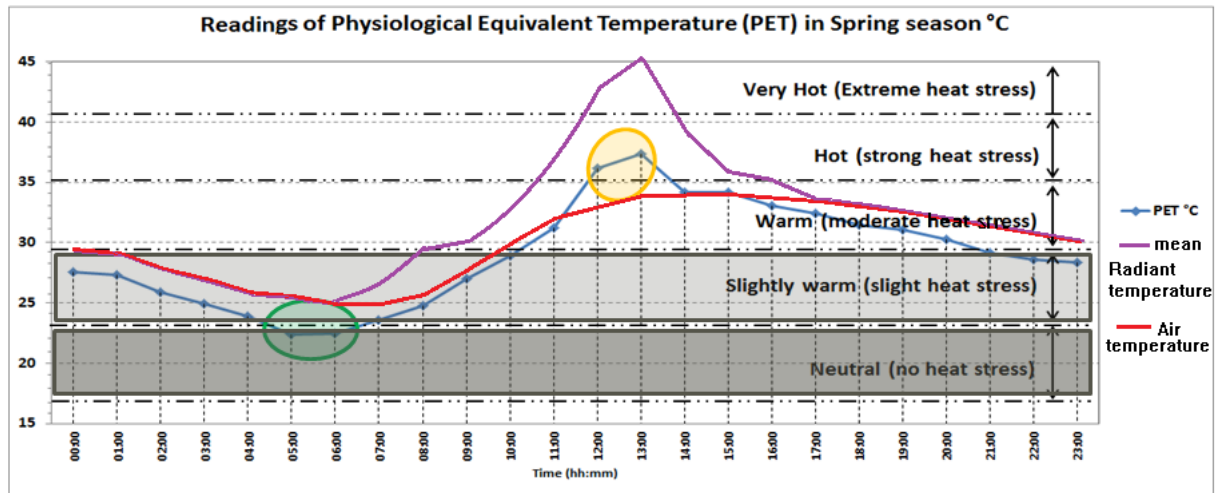

FIG. 2: The PET index indicates that people feel slightly warm before 10 a.m. with slight heat stress. Strong heat stress occurs when air and radiant temperatures reach peak time between 12 to 1 pm.

According to Abdel-Ghany et al. (2013), thermal discomfort is mainly caused by heat load exchanges between pedestrians and the surrounding urban interventions through radiation, convection and evaporation modes. In other words, "the variation of mean radiant temperatures above the air temperature has its impact on human physiology and subsequently thermal discomfort, particularly in hot environments with low humidity and wind velocity" (Al-Ghamdi, 1993:94).

However, the complexity of intangible urban fluid flows (e.g. air and radiant temperatures, relative humidity and air speed) inside and around buildings has posed challenges to architects and urban designers for designing better environments, such as designing thermally comfortable public spaces for indoor and outdoor environments, especially in hot climates. "Computational fluid dynamics, usually abbreviated as CFD, is a branch of fluid mechanics that uses numerical methods and algorithms to solve and analyze problems that involve fluid flows" (Masnavi et al., 2012:117). Integrating CFD into urban design processes opens the potential of visualizing air flows and heat transfer patterns (i.e. mimicking fluid flows) and its effects on the urban environments. It can provide the main microclimatic parameters that can enable the calculation of human thermal comfort, with the distribution of thermal comfort sensation (e.g. Predicted Mean Vote index, PMV, Standard Effective Temperature, SET*, etc.).

This research highlights the CFD guidelines and the potential of adopting CFD as a simulation technique to investigate the complex fluid flows in urban thermal environments. It discusses the advantages and limitations of CFD tools. It describes the CFD simulation approach and the procedure for conducting CFD simulation. This paper also gives examples of case studies of CFD assessment for indoor and outdoor urban environments, and the practical use of RANS solver in comparison with LES, DES, and DNS models. Finally the paper highlights a case study of a CFD simulation of an urban street in the hot arid city of Madinah, Saudi Arabia.
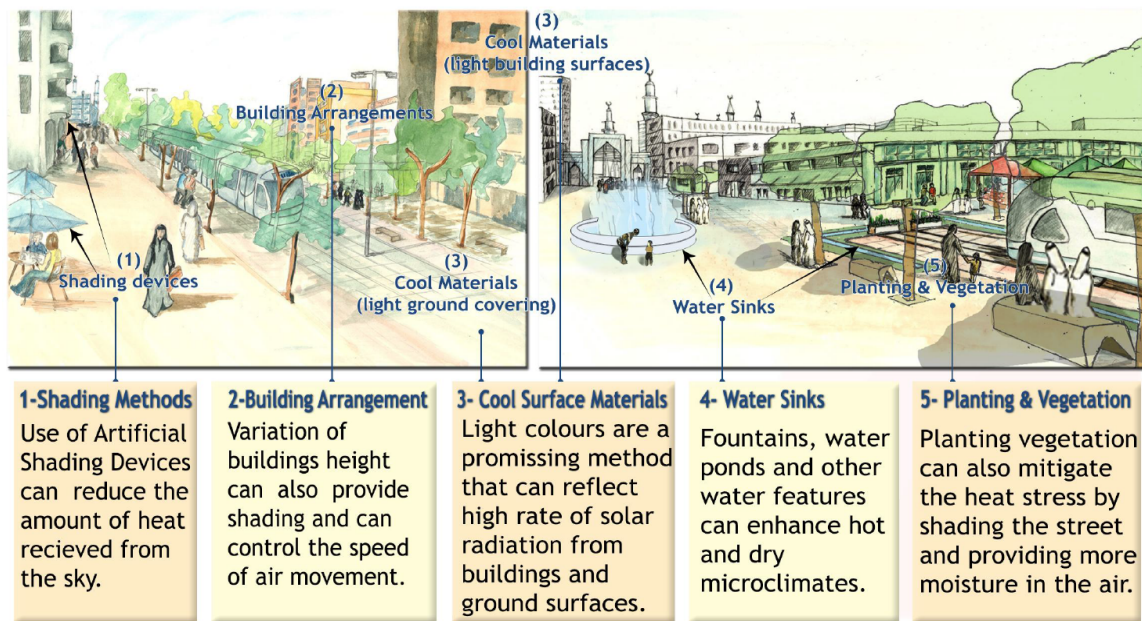
FIG. 3: Urban microclimatic interventions for hot dry urban environments. (source: the authors).

2. ANALYTICAL TECHNIQUES FOR THERMAL COMFORT

Different approaches are used to assess urban heat islands (UHI). The metrological technique for the assessment of thermal comfort involves an analysis of urban-rural differences such as thermal variations, air velocity, turbulence, and pollution concentration, based on data collected by mobile stations. The advantage of this approach is that it is relatively easy to carry out, however only a limited number of parameters can be measured simultaneously, and it is not always possible to produce a 3D spatial distribution of the relevant factors in an urban environment. The process can also be time consuming and costly (Mirzaei and Haghighat, 2010). This data is then used in analyzing the spatial and UHI within a city. This is combined with adaptive thermal comfort predictions, including observational approaches and simulation methods to study the mutual effect of the increased ambient temperatures and possible adaptive behaviors used by pedestrians and users of urban space (Mirzaei and Haghighat, 2010).

Voogt and Oke (2003) suggest that UHI can be evaluated using thermal remote sensing, which involves the remote observation of UHI using satellites and aircraft. This technique can provide data on surface temperature, the effects of surface radiation, and thermodynamic properties. The disadvantages of this technique are that it is very expensive, and because of atmospheric interactions it is not always possible to obtain steady images of the urban surface. However, another technique is to use small scale modeling in which a prototype of the urban area is constructed, and tested using a wind tunnel. The difficulty in this technique is creating an accurate model and the process can be expensive. It is acknowledged, however that this technique can be useful in studying some impacts of the building on its environment, such as visual impact or pollution dispersion (Poreh, 1996).

An alternative technique is to use simulation models, such as energy balance models, computational fluid dynamics (CFD), meso-scale models, and micro-scale models. Energy balance models take account of the energy exchanges with surfaces and ambient air in the urban canopy. These models can be used to predict the ambient temperatures and surfaces temperatures of buildings, pavements and streets. These types of models are quick to run and can provide accurate results. However, according to Mirzaei and Haghighat (2010), the major drawback of this technique is the absence of air velocity, and it separates temperature and velocity fields, such that the assumptions used do not always accurately represent the interaction of velocity and temperature in reality.

On the other hand, CFD simulations can predict the important urban microclimatic parameters in cities, with the aim for understanding urban aerodynamics system and fluid flow in and around buildings, so that heat gain and pollution concentration can be mitigated and/or to produce better cross-ventilation for human comfort (Chung and Choo, 2011). CFD is a modeling technique originally established as a simulation tool for mechanical engineering, however, it has also been used as a tool for assessing the internal environment of buildings and its relations with the building envelope, and for evaluating buildings' outdoor environments (Erell et al., 2011:214). The applications of this technique are described further in the following sections.

3. ADVANTAGES AND LIMITATIONS OF CFD MODELING

Owing to the increasing density of urban development and high-rise buildings in cities, the energy demand increases. The urban microclimates in cities face significant changes in the atmospheric characteristics, as a result of trapped radiant heat, intensified pollutants and obstructed winds, which can lead to thermal discomfort (Mirzaei and Haghighat, 2010). These phenomena can modify the local wind patterns, humidity and ambient temperatures. The advantage of CFD is that it can be used to evaluate a range of issues comprising air speed and movement, air quality and pollution diffusion, wind comfort and thermal comfort as well as the effects of relative humidity and vegetation on indoor and outdoor spaces (Blocken and Persoon, 2009; Tominaga and Stathopoulos, 2009; Chung and Choo, 2011). The other advantages of CFD software compared to wind tunnel and full-scale measurements include: being readily available, inexpensive, enables changes easily with no restrictions and analyzes complex environmental problems.
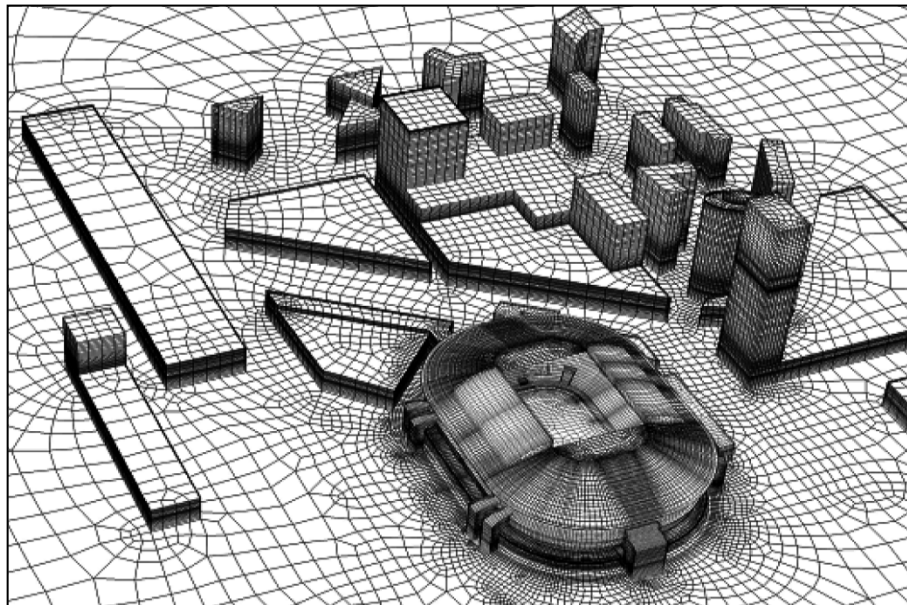

FIG. 4: An example of geometrical model and computational grid for CFD.
Source: Blocken and Persoon (2009).

However, CFD is reckoned to be a complex method in terms of calculating all the relevant fluxes with a high resolution of computational grids, an example of computational meshing is illustrated in Fig. 4 above (Blocken and Persoon, 2009). The finer the meshes/grids are used the more accurate results it can give. There are four basic 3D cell types for meshing in CFD, which are: tetrahedral, pyramidal, prismatic and hexahedral cells. Careful selection of appropriate cell types is important for both computational power and accuracy of the results.

According to Erell et al. (2011:214), CFD models entail "validation, and due to the shortage of well-documented high-quality data from field studies, this remains a major drawback of most urban climate models." It requires large computational power and knowledge of the governing equations to interpret the results. Different scales of turbulence in an urban environment require separate modeling and simplified simulation, which may result in inaccurate outcomes (Chung and Choo, 2011).

4. CFD MODELING APPROACH

There are four major turbulence modeling approaches in CFD including Reynolds Averaged Navier Stokes (RANS), Large Eddy Simulation (LES), Detached Eddy Simulation (DES) and Direct Numerical Simulation (DNS).

The Reynolds Averaged Navier Stokes (RANS) approach is a modeling method in which the major variables such as temperature and velocity are divided into time-averaged and turbulent fluctuation, and then the turbulent model is used to model the turbulent fluctuation (Nielsen et al., 2007). Blocken and Persoon (2009) used RANS in studying an urban setting to evaluate wind comfort on pedestrian level around a large football stadium to study the effects of adding new high-rise buildings in the surroundings. The advantages of RANS include its availability in all CFD codes, inexpensive and widely validated, but it is not as accurate as LES because of the lack of capturing smaller length scale (eddy scale) in RANS. Blocken et al. (2009) and He and Song (1999) indicated another shortfall of RANS, which is that RANS solves only the mean flow and small eddies, whereas the LES solves the large and most important turbulent eddies. Santiago et al. (2010) have used LES model and RANS model to evaluate the effect of the direction of incident wind on the flow plume dispersion. It was noticed that LES requires greater computational cost than RANS, and the use of RANS with turbulent kinetic energy (k-ε) model is reasonably suitable for simulating wind flow in urban environments, and has increasingly been used for wind studies at pedestrian level (e.g. Blocken et al., 2004; Yoshie et al., 2007; Blocken and Persoon, 2009).

In LES model, large scale structures in turbulent flow are created directly, this is due to unsteadiness of the mean flow (shear or buoyancy effects) that are simulated directly as they are problem reliant, anisotropic and play a key part in transportation of mass, momentum and energy. LES modeling is most appropriate for the simulation of air pollutant, which is because of its ability to solve the large eddies in the field of the fluid flow (e.g. Walton et al., 2002). In contrast, small scale structures can be modeled in LES with less effect on the prediction value (Uddin, 2008). The grids in LES are more refined compared to RANS and hence need more computational power for simulation. The employment of LES in urban environment studies could be seen in Salim et al. (2011), Li et al. (2009), and Tominaga, et al. (2008). Researchers such as Tominaga et al. (2008) applied LES simulation to high-rise building geometry to study the wind flow around it within the surface boundary layer, flow within an urban complex and around a tree.

The introduction of Detached Eddy Simulation (DES) was prompted by the quest to address the challenge of high–Reynolds number, immensely separated flows. Epstein et al. (2011) have used DES solver (in their study on modeling a new approach to evacuation planning) to avoid RANS's known weaknesses for heavily separated flows. It combined the ideas of both LES and RANS in addressing the simulation problem because of the fact that each of them cannot solve the problem on their own (Spalart, 2009). On the other hand, Direct Numerical Simulation (DNS) is the most accurate technique of solving fluid turbulence. In this method, the Navier-Stokes equations are solved using a fine mesh when all the spatial and temporal scales available in the flow are resolved (Sengupta and Mashayek, 2008). This approach to turbulence simulations solves the Navier-Stokes equations without any approximation of the turbulence except numerical discretization (Furbo et al., 2009).

In general, the responsibility of a turbulence model in CFD simulation is to close the RANS equations by computing the components of the Reynolds stress tensor (Catalano and Amato, 2003). There are different RANS turbulence models, including k-ε Turbulence model, k-ε RNG model, k-ε realizable model, k-ω model, Algebraic stress model, Non-linear models, the SST (Shear Stress Transport) model etc., the selection of these turbulence model for simulation is purely context based. Turbulence model that applicable in certain flow problem cannot be appropriate in others. That is why, sensitivity analysis among available turbulence models is essential to select the best one that can solve the problem at hand with less error.

In a CFD study by Ramponi and Blocken (2012) for the simulation of cross-ventilation for a generic isolated building, the researchers have used 3D steady RANS equation as a solver, coupled with the shear-stress transport (SST) k-ω model. The pressure-velocity coupling was governed by the SIMPLE (Semi-Implicit Method for Pressure-Linded Equations) algorithm and both the pressure interpolation and discretization schemes were second-order for both the convection and the viscous terms equations. An assumption was made for convergence based on the CFD code Fluent guide (Fluent 6.3, 2006) that the result to be obtained when the whole scaled residuals levelled off and reached a minimum of 10-6 for x, y and z momentum, 10-5 for k and 10-4 for ω and continuity.

Janssen et al. (2013) have studied the pedestrian wind comfort around buildings using RANS equation and the realizable k-ε model to provide part of the aerodynamic information (i.e. related contributions of both the terrain and the design). Pressure velocity-coupling was also used in their research governed by SIMPLE algorithm. Second-order discretization schemes were used for the same terms that Ramponi and Blocken have mentioned above. They have performed a high-resolution grid for the CFD simulations based on the analysis of grid-sensitivity, and obtained convergence when the residuals reached the following minimum values: x-, y-, and z-momentum: 10-8, k and ε: 10-7 and continuity: 10-6.

They found that the 3D steady RANS approach is considered to be more appropriate modeling method than LES simulation for wind comfort studies in a complex urban environment with high wind amplification factor. The researchers indicated that "the amplification factor U/U0 (which is the ratio of the local pedestrian-level wind speed U to the wind speed U0 that would occur at the same position without buildings) is generally predicted with a high accuracy of 10-15% in the regions where U/U0 > 1, while the predicted wind speed is generally significantly underestimated by CFD where U/U0 < 1, at some locations by a factor 5 and more" (2013:548). In addition to this, 3D steady RANS approach is suitable for pedestrian-level wind flow studies when performing simulation for many wind direction (e.g. 12 or 16 directions), as the process requires repetition for configurations with remedial measures implemented (Yoshie et al., 2007).

Murakami et al. (1999) have conducted a coupled analysis of CFD and radiation simulation, using the following four coupled equations: transport equation of momentum; transport equation of heat; transport equation of moisture; and heat transfer equation by radiation. The researchers have employed periodic boundary condition for the assessment of outdoor thermal comfort and the effect of plants canopy model on pedestrian relaxation. They have considered the effects of drag force of the planted trees; the effects of shading on shortwave and long-wave radiations; and the production of latent heat from the plant canopy. The researchers have used a revised k-ε model with modification of LK (Lanunder and Kato) model to include the correct buoyancy effects on sensible and latent heat fluxes. The computation of radiative heat transport was processed through using the method based on the Monte-Carlo simulation. The distribution of standard effective temperature (SET*) index was calculated separately, using the data obtained from CFD, to predict the human thermal comfort conditions.

5. PROCEDURE FOR CONDUCTING CFD SIMULATIONS

The CFD simulation procedure starts with the creation of the building or system geometry, followed by grid generation and then mathematical solution of the problem via simulation.

CAD software or built-in geometric modelers that are included in various CFD programs can be used to create the building as a geometric representation. After finalizing the geometry, a grid/mesh will be generated using a standalone meshing software, or build in meshing tools within the CFD package. Among the Common grid generation programs are Harpoon by Sharc; Gridgen by Pointwise; ANSYS Mesh; BOXERMesh by Cambridge flow solutions; etc. The grids are generated using structured Cartesian grids, structured body-fitted grid or unstructured grids (Nielsen, et al. 2007). When the grid/mesh generation is completed, the turbulence model, material characteristics, cell zone conditions and boundary conditions will be set. The boundary conditions required for each object in the model including parameters such as velocity, pressure, temperature, etc. will be set. The next parameter after the boundary condition is the solution monitors to set the convergence criteria in terms of iterations in the scaled residuals.

A CFD solution technique uses iterative or repetitive process to continually improve on a solution (NAFEMS, 2013). The code will continue repeating the solution until convergence is reached. The condition for monitoring solution convergence in steady state is different from that of transient CFD simulation. In steady state simulation, a solution is said to be converged when the lines of convergence plot stop varying and slope becomes zero (e.g. Fig. 5). However, in transient simulation convergence is monitored based on engineering judgments (Autodesk, 2011). Finally, the solution is initialized and calculation is run.

The results obtained are processed using in-built or standalone post-processing programs. These programs are capable of providing both qualitative and quantitative outputs. The qualitative results are visualized in form of graphics and animations. Some of the most common graphics tools include contours, vectors, pathlines, particle tracks and mesh, while the most common animation tools include sweep surface, scene animation and solution

animation playback. However, the quantitative results are obtained through XY plots, histograms, fluxes, forces, surface integrals, and volume integrals etc.
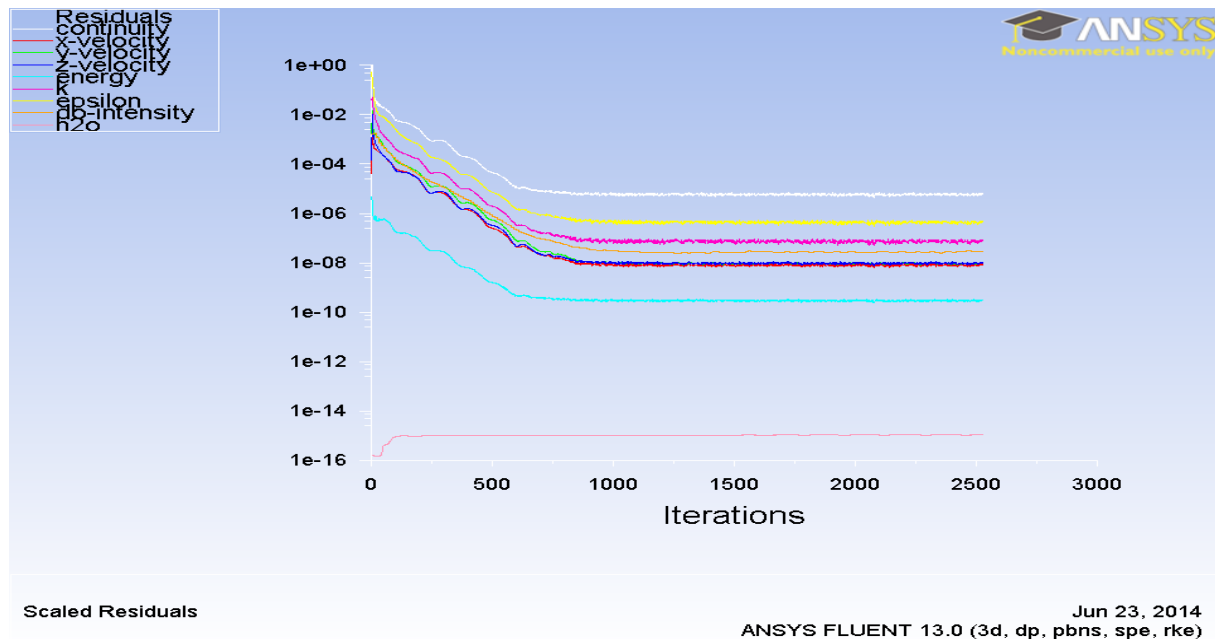

FIG. 5: A solution is said to be converged in a steady state simulation when the lines of the convergence plot stop varying and the slope becomes zero. (Source: the authors).

6. CFD PRACTICAL GUIDELINE

The assessment of an urban environment using computational fluid dynamics (CFD) could either involve an indoor or outdoor evaluation of the environmental quality such as the air quality and thermal comfort. Many studies have been conducted using CFD to evaluate indoor and outdoor environmental conditions. These studies have cut across various environmental conditions such as air quality, thermal comfort, and airflow characteristics in urban indoor and outdoor environments. Cheng and Zang (2004) studied the use of CFD tools for indoor environmental design and stressed the importance of proper validation studies, grid independence studies and proper handling of complex boundary conditions. Furthermore, CFD tool has been used extensively to evaluate Natural ventilation of indoor environments (Van Hoop and Blocken, 2013; Cook, et al. 2005; Yang, 2004, Mohammed et al. 2013, Meroney, 2009). However, many studies have also been conducted in the context of outdoor urban environments. CFD tool has been used by Blocken et al. (2012) to simulate pedestrian wind comfort and wind safety in urban areas (as shown in figure 4 above) and confirmed the considerable advantages of CFD compared to wind tunnel testing. McAlpine and Ruby (2004) in their study of air quality in microenvironments acknowledged the capability of CFD tools in allowing more accurate predictions. Moreover, Gousseau et al. (2011) also used CFD tool to study near-field pollutant dispersion in an urban environments, focusing both; on the prediction of pollutants concentration for pedestrian outdoor air quality and on building surface for ventilation system inlet and indoor air quality.

A best practice CFD guideline for the simulation of flows in urban environment was proposed by European Cooperation in the field of Scientific and Technical Research (COST) (Franke et al., 2004; Franke 2006; Franke et al., 2007). Researchers have used CFD tool to simulate pedestrian wind comfort and safety in urban environments (Blocken et al. 2012); and to simulate the effects of implementing bioclimatic-design applications in the urban environment coupling with thermal comfort index (Stavrakakis et al., 2012).

6.1 Computational Domain

Tominaga et al. (2008), researchers in the Working Group of the Architectural Institute of Japan (AIJ), have proposed guidelines for practical applications of CFD to pedestrian wind environment around buildings, which

are based mainly on high Reynolds number (Re) of Reynolds Averaged Navier-Stokes equations (RANS) models. The researchers have used several models of k–ε, DSM and LES (Large Eddy Simulation) in order to obtain the results of wind flow around a high-rise building within the surface boundary layer, flow within a building complex in an actual urban environment, and flow around a tree. Based on the knowledge of wind tunnel experiments it has been suggested that for the size of the computational domain the blockage ratio, around the target building and the surroundings, should be 3% or below, with the boundary distance of at least 5H (i.e. 5 times the tallest building height) away from a 3D building on all directions, except from the outflow boundary that should be at least 10H (as suggested by Mochida et al., 2002; Shirasawa et al., 2003; cited in Tominaga et al., 2008:1751). Research in COST (by Franke et al., 2007) has also recommended similar dimensions for most of the computational domain boundaries, especially for the inflow and the side boundaries, and the outlet boundary of 15H was suggested. Researchers such as Janssen et al. (2013) have considered these best practice guidelines for the dimension of the computational domain (5H × 5H × 5H × 15H) to simulate pedestrian wind comfort around buildings. The computational region should represent the surroundings with at least a street block in each direction around the interest site to gain realistic results (Yoshie et al., 2006). For the representation of surroundings, a radius of 1-2H from the target construction is generally acceptable for the modelling to give realistic results (Tominaga et al., 2005). According to Franke (2006) greatest level of detail is required in the central area of the study but less detail should be represented in the surroundings.

For the simulation of thermal comfort levels in an urban environment in Greece, Stavrakakis et al. (2012) have specified the computational domain with a distance of 4H for the lateral and the upper boundaries from the building complex, while the boundary for the outlet located 8H far from the area of interest. The discretisation of the computational domain applied in the study was a non-uniform unstructured grid, with approximately grids' control volumes of 350,000 for the actual urban complex, and 450,000 for after introducing architectural interventions to the domain, whilst 0.2m was reached for the scale of spatial resolution near small wall surfaces. Van Hooff and Blocken (2010) have studied the thermal effects and wind flow pattern in and around a large stadium in Amsterdam, using the domain dimensions that are recommended by Franke et al. (2007) and Tominaga et al., (2008), with maximum blockage ratio of 1.6% (i.e. below the recommended maximum of 3%).

6.2 Grid Discretisation

For the accurate prediction of the flow pattern around a building in an urban environment it is important that the characteristic of separating flows near walls and the roof to be reproduced correctly. Tominaga et al. (2008) indicated that to reproduce this separation around the upwind corners of a targeted building, the minimum of 10 fine grids on one side of the building should be arranged. It is also recommend applying stretching ratios of maximum of 1.3 (Franke et al., 2007; Tominaga et al., 2008) or even less than 1.2 (Bartzis et al., 2004) of adjacent grids to set up grid shapes with similar widths, especially in areas with a steep velocity gradient. However, it is advised to test the sensitive of the results of using this stretching ratio on mesh resolution, as it may change according to the building shape and the surroundings (Franke et al., 2007).

Moreover, Franke et al. (2004) assert that regarding the cell resolution for actual building the calculation of wind speed at pedestrian height of 1.5 – 2 meters should be arranged at the 3rd or 4th grid higher from the ground surface, with 10 grids at least to be set to building side and other 10 per building geometry. This is comparable to the AIJ guidelines where it is stated that the cell location should be set to at least at the third or above from the height of the ground surface, with the minimum resolution grid of about 0.5 – 5 meters within the area of interest (i.e. one tenth of the building scale) (Tominaga et al., 2008). Janssen et al. (2013) have implemented 5 cell layers below the pedestrian height (i.e. 1.75m) based on a detailed a grid-sensitivity analysis for the simulation of pedestrian wind comfort around buildings. A grid-sensitivity analysis that the researcher have constructed are additional grids of a coarser mesh with 2,598,602 cells, and a finer mesh with 12,392,255 cells. Regarding this additional cells the researchers have found that there were significant differences in wind speed between the coarser grid and the basic grid, whereas small differences were between the finer and basic grids. This indicates that the basic grid should be used as it is validated for the accuracy and computational cost.

6.3 Boundary Conditions

Boundary conditions is "a condition that is required to be satisfied at all or part of the boundary of a region in which a set of differential equations is to be solved" (Barton and Babister, 2012). An illustration of the

computational domain with building models for CFD simulation of atmospheric boundary layer is shown in Fig.6, which demonstrates the three main parts of domain, including upstream, central, and downstream parts (Blocken et al, 2007). Franke et al. have recommended using symmetry boundary conditions for the lateral and top boundaries. This would enforce a parallel flow by forcing the velocity component normal to the boundary.

According to Blocken et al. (2012) and Priyadarsinin et al. (2008), the specification for inlet flow boundary of the computational domain requires profile conditions of neutral vertical wind velocity profile U on flat terrain, vertical distribution of turbulent kinetic energy k, and turbulent dissipation rate ε; whereas the outlet boundary requires free pressure specification with zero static pressure. The researchers have also highlighted the lateral and upper surfaces conditions of computational to be specified by symmetry boundary conditions (i.e. zero normal velocity and gradients).
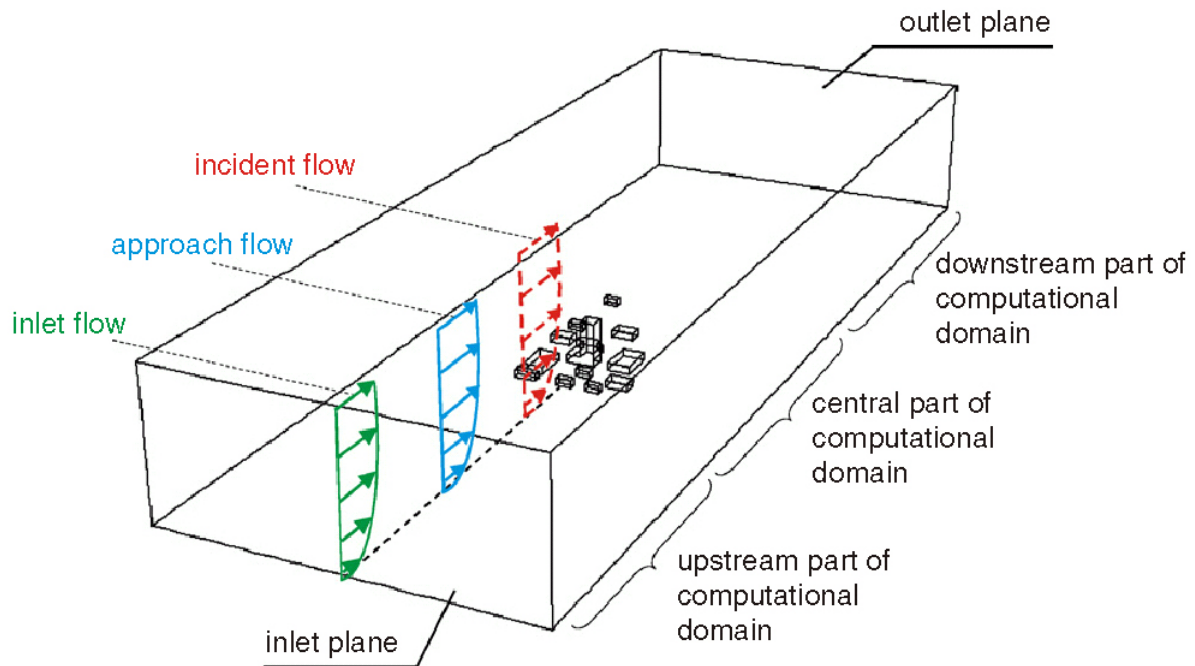

FIG. 6: Main parts of the computational domain for roughness modeling. Source: Blocken et al. (2007)

The equations for the U, k and ε according to the Japanese Architectural Institute, AIJ, are as shown below (Eqn 1; 2; and 5). The equation for U is based on Zoumakis and Kelessis (1991) calculated with the power-law exponent determined by the terrain category. However, U can also be calculated based on the aerodynamic roughness length z_0, as is shown further in equation no. (6) (Wieringa, 1992).

$$U_{(z)} = U_{ref} \left(\frac{z}{z_{ref}} \right)^{\alpha} \tag{1}$$

$$k_{(z)} = \frac{\sigma_{u(z)}^2 \quad + \quad \sigma_{v(z)}^2 \quad + \quad \sigma_{w(z)}^2}{2} \tag{2}$$

where $U(z)$ is the wind speed at height (z), (U_{ref}) is the wind speed at reference height z_{ref} (i.e. the height of the meteorological station), and the power-law exponent α is a function of both the atmospheric stability and the terrain surface physical characteristic. In addition, σ_u, σ_v and σ_w are the three directions of standard deviations or so called the RMS value of velocity fluctuation.

And the squared standard deviation of the stream-wise direction $\sigma_{u(z)}^2$ at a specified height z can be calculated using the longitudinal turbulence intensity equation ($I_{(z)} = \sigma_{u(z)}/U_{(z)}$), which is determined by the boundary layer height z_G above the terrain category, as follows:

$$\sigma_{u(z)}^2 = \left(I_{(z)}\, U_{(z)}\right)^2 \tag{3}$$

$$I_{(z)} = 0.1 \left(\frac{z}{z_G}\right)^{(-\alpha-0.05)} \tag{4}$$

The researchers recommend that the $\varepsilon_{(z)}$ to be calculated by assuming the dissipation rate to be equaled to the production term $P_{k(z)}$ for the kinetic energy $k_{(z)}$ equation at the height z. Thus the formulation for this, based on the model empirical constant (C_μ=0.09), is as follow:

$$\varepsilon_{(z)} \cong P_{k(z)} \cong -\overline{u'w'}\frac{dU_{(z)}}{dz} \cong \sqrt{C_\mu}k_{(z)}\frac{dU_{(z)}}{dz} \tag{5}$$

However, it should be noted that the equations that are based on the velocity profile (Eqn. 1) mentioned above are calculated by the power-law exponent determined by wide range of terrain categories. It does not calculate the effects of the aerodynamic roughness length (z_0) underlying the flow pattern on a specified height (z), which might be important in estimating specific microclimatic parameters for the thermal comfort studies. Nevertheless, either the use of wind profile that is expressed by the power-law exponent or by the aerodynamic roughness of the implicit terrain, it "should be representative of the roughness characteristics of that part of the upstream terrain that is not included in the computational domain (i.e., the terrain upstream of the inlet plane" (Blocken et al., 2007:239). The velocity profile U at specified heights z, and roughness length z_0 has been validated in COST (Franke et al., 2004), WMO (Oke, 2006) and Blocken et al. (2012), which takes into account the von Karman constant ($\kappa = 0.42$; constant shear stress with height), which is calculated within the low portion of the atmospheric boundary layer ($_{ABL}$) (0-200m) only, with the friction velocity (U*), is as follows:

$$U_{(z)} = \frac{U_{ABL}^*}{\kappa}\ln\left(\frac{z+z_0}{z_0}\right) \tag{6}$$

Many researchers, including Janssen et al. (2013), have implemented this formula of wind profile in CFD for wind studies at pedestrian height, as well as turbulence kinetic energy and turbulence dissipation rate that are linked to the roughness length parameter. According to Blocken et al. (2007), the roughness of the implicit terrain, in the upstream and downstream parts of the domain, is either expressed in z_0 (i.e. the aerodynamic roughness length, in the range 0.03-2m), or in terms of the equivalent sand-grain roughness height for the atmospheric boundary layer ($k_{S,ABL} \approx 30z_0$, in the range of 0.9 to 60m). The latter is less often applied to the bottom of the domain due to its large-scale. However, the researchers have stated that in the centre part of the computational domain, where it explicitly models the actual geometrical terrain, the roughness is most often expressed in terms of the equivalent sand-grain roughness height (k_S, in the range of 0-0.1m). These researchers argue that if this roughness type is used in the wall functions, then the following four requirements should be satisfied simultaneously:

- High mesh resolution should be used sufficiently in the vertical direction within one meter of the cell height in the bottom layer of the domain, or according to Franke et al. (2004) structuring 2 to 3 layers bellow pedestrian height (1.75m);
- A horizontally homogeneous ABL flow is required in the upstream and downstream areas by using a wall function;
- Distance (z_P) from the center point (P) of wall-adjacent cell to the bottom wall of the domain should be kept larger than the sand-grain roughness height (k_S); and

- The relationship between the roughness of the sand-grain (k_S) and the aerodynamic roughness length (z_0) is important to be identified; concerning "the relationship that results from matching the ABL mean velocity profile and the wall function in the CFD code".

The equation (6), which was proposed by Richards (1989) based on the Harris and Deaves (1981) mathematical model, agrees with the computational domain height that is usually lower than the height of the atmospheric boundary layer. Based on the reference height z, the kinetic energy $k_{(z)}$ can be calculated using the inlet longitudinal turbulence intensity ($I_{(z)}$) and the mean wind speed, Eqn. 7 (also refer to Eqn. 3 and 4).

$$k_{(z)} = \sigma_{u(z)}\left(I_{(z)}U_{(z)}\right)^2 \tag{7}$$

Blocken et al. (2012) suggest to assume the standard deviations of the turbulent fluctuations in the three directions are the same ($\sigma_u = \sigma_v = \sigma_w$), which means $\sigma_{u(z)} = 1.5$. Tominaga et al. (2008) recommend that $\sigma_{u(z)}=1$, which is given by assuming $\sigma_u = \sigma_v + \sigma_w$. According to Ramponi and Blocken (2012), this value of standard deviation is very sensitive (it is generally in the range between 0.5 and 1.5) as it was found that wind speed decreases by 7% when it is increased from 1 to 1.5, and the speed increases by 12% when it is decreased from 1 to 0.5. Moreover, Janssen et al. (2013) has stated that the ranges of inlet longitudinal turbulence intensity ($I_{(z)}$) for $z_0 = 1$ are from 39% at pedestrian height to 8% at gradient height. For $z_0 = 0.5$m the $I_{(z)}$ ranges are from 29% at pedestrian height to 5% at gradient height. Van Hooff and Blocken (2010) agree that the value for the aerodynamic roughness length z of the surroundings is recommended to be determined (by wind direction) within the radius of 10 km based on Wieringa (1992).

The turbulent kinetic energy $k_{(z)}$ can also be estimated using the ABL friction velocity $U*_{ABL}$ and a model constant C_μ of the standard k–ε model, Eqn. 8 (Blocken et al. 2007), which is simplified, according to the height of the computational domain being in the lower part of the ABL, by Richards and Hoxey (1993) that is based on the Harris and Deaves (1981); dissipation rate is also given in Eqn. 9 based on ABL friction velocity:

$$k_{(z)} = \frac{U_{ABL}^{*2}}{\sqrt{C_\mu}} \tag{8}$$

$$\varepsilon_{(z)} = \frac{U_{ABL}^{*3}}{\kappa(z+z_0)} \tag{9}$$

$$U_{ABL}^* = \frac{\kappa U_z}{\ln\left(\frac{z+z_0}{z_0}\right)} \tag{10}$$

These profiles are often used as inlet profiles for CFD simulations when measured profiles of U and k are available, otherwise it can be used without integrating the roughness length value as proposed by Durbin and Petterson Reif (2001; 2011), which with the latter case "the profiles for k and ε are converted into profiles for either the specific dissipation rate ω ($\omega_{(z)} = \varepsilon_{(z)} /C_\mu k_{(z)}$), the turbulent viscosity ratio μ_t/μ or the Reynolds stresses" (Blocken et al., 2007:242). An example for the use of specific dissipation rate is provided by Ramponi and Blocken (2012) for the study of cross-ventilation for a generic isolated building. While the inlet vertical velocity profile proceeding towards the outlet boundary, it changes gradually with the characteristics of the urban and natural features. Therefore, it is important to specify the boundary conditions of these features surfaces, including the ground, building walls, etc., to minimize the changing effects (Tominaga et al., 2008).

Researchers such as Stavrakakis (2012) have conducted a special CFD simulation study to quantify microclimate and comfort conditions in urban thermal environment. They have made five main assumptions for the simulation, which are: "incompressible flow of a Newtonian fluid; neutral atmospheric conditions; Richards-Hoxey assumptions for the Atmospheric Boundary Layer (ABL) (Richards & Hoxey, 1993); the fluid is considered as a mixture of dry air and water vapour […]; and traffic conditions in the area are currently neglected and only the effect of construction materials and physical elements is taken into account" (p.6). The

researchers have specified the exponential law for the velocity profile at the inlet boundary conditions for two wind directions (U_X and U_Y), however the equations (Eqn. 11 and 12) obtained by the combination of velocity formulation at Atmospheric Boundary Layer height (z_{ABL}; 300m from the ground) and at a reference height z_{ref}.

$$U_X = \frac{U_{ref} \sin\widehat{\theta}}{\left(\frac{z_{ref}}{z_{ABL}}\right)^\alpha} \left(\frac{z}{z_{ABL}}\right)^\alpha \tag{11}$$

$$U_Y = \frac{U_{ref} \cos\widehat{\theta}}{\left(\frac{z_{ref}}{z_{ABL}}\right)^\alpha} \left(\frac{z}{z_{ABL}}\right)^\alpha \tag{12}$$

where U_X and U_Y are the velocity component at X and Y directions, respectively, z_{ref} is the reference height, e.g. the metrological station height, U_{ref} is the velocity of incoming wind, α is the terrain roughness, z is an arbitrary height from ground, and $\widehat{\theta}$ is the wind incidence angle.

The researchers have used the turbulence components based on the Richards-Hoxey assumptions for the atmospheric boundary layer, which are imposed using the following equations (Eqn. 13 and 14):

$$k_{(z)} = \frac{U_\tau^2}{\sqrt{C_\mu}}\left(1 - \frac{z}{z_{ABL}}\right) \tag{13}$$

$$\varepsilon_{(z)} = \frac{U_\tau^3}{\kappa z} \tag{14}$$

where U_τ is the wall-function friction velocity which can be calculated by using the shear stress at the wall (τ_w) and the fluid density (ρ), C_μ is the turbulent viscosity coefficient, and κ is the von Karman constant.

$$U_\tau = \sqrt{\tau_w/\rho} \tag{15}$$

$$\tau_w = \frac{f\rho U_{ABL}^2}{2} \tag{16}$$

$$f = 0.045 \sqrt[4]{\left(\frac{\mu}{\rho\ U_{ABL}\ z_{ABL}}\right)} \tag{17}$$

where f is the friction coefficient calculated by the Blasius equation, U_{ABL} is the velocity at the ABL height ($U_{ABL} = U_{ref}\left(\frac{z_{ABL}}{z_{ref}}\right)^\alpha$), and μ is dynamic molecular viscosity.

7. CASE STUDY OF A HOT DRY URBAN STREET CONDITION

Field studies were conducted in Madinah, Saudi Arabia at three selected sites with varied urban densities and heights exist (i.e. Quba street, which is 3km long) (Fig. 7), to measure the four main microclimatic parameters for the assessment of outdoor pedestrian thermal comfort, including the measurements of air temperature, globe temperature (which is used for the calculation of mean radiant temperature), relative humidity and air velocity. The three measuring stations were located 1) near the city center of Madinah city (near the most visited site in the city called the Prophet's Mosque) with high urban density area; 2) near Quba mosque in the southern part of the city, with a comparatively low urban density area; and 3) at a point along Quba Street in between these two mosques (a medium urban density area). All three sites chosen as case study areas are situated between the two

mosques and are characterized by buildings used for a combination of residential purposes (above street level) and retail purposes (street level). In the current research, the simulation study was conducted on the high urban
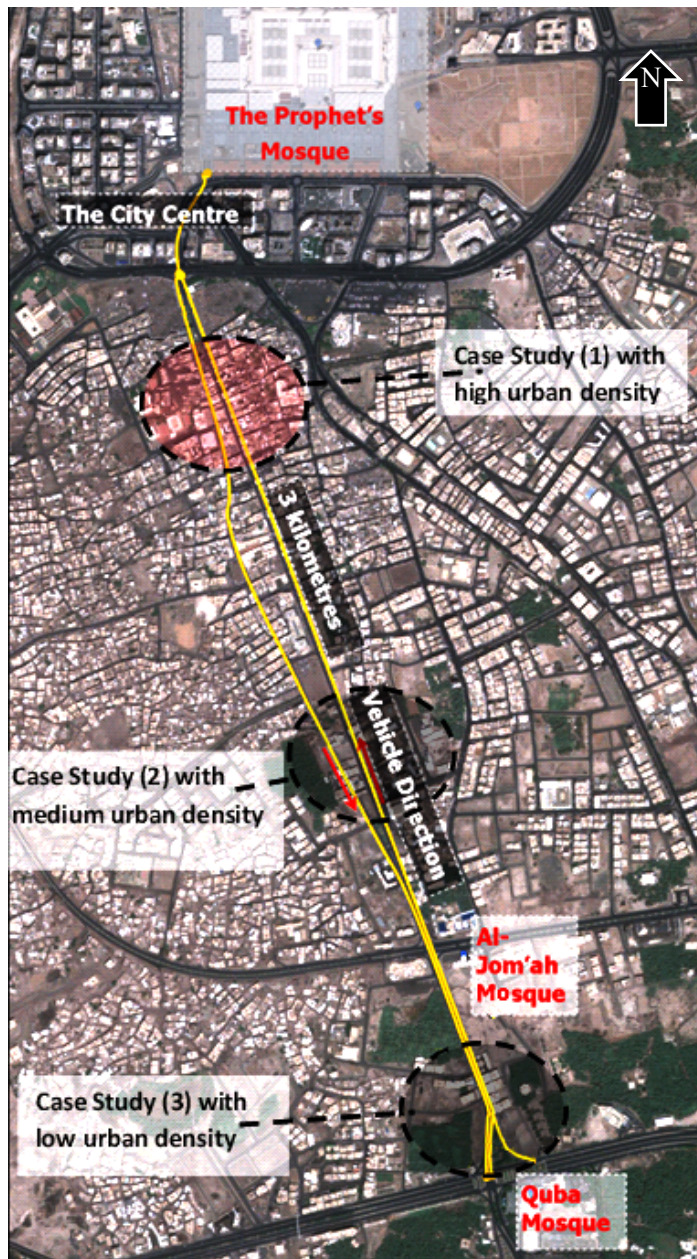

 FIG. 7: The three case studies locations with different urban densities selected along Quba road.

density area only. It has to be acknowledged that only the height of buildings and orientation of street have been examined for the case study, whereas other urban microclimatic interventions such as the vegetation, ground and building surface materials, and water features have not been examined in this paper.

The field measurements were conducted during all four climatic seasons of the year for the duration of two weeks per season and around the clock (24 hours). For this paper, only the data collected in April 2013 (spring season) for the high urban density area was simulated with the aim of extending the possible use of outdoor space in non peak summer conditions. The selected high urban density area is presented in Fig. 8a, centered by a field measurement location point where the mean air temperature was about 30°C, relative humidity of 17% and air velocity of 0.7. The 3D geometry (Fig. 8b) and the meshing (Fig. 8c) were processed using Ansys DesignModeler and Ansys Meshing tools, respectively. The use of CutCell meshing process was selected for the

urban environment, using coarse cells, as the proximity and curvature type that are characteristic of this type of environment gave better results compared to other meshing properties. The number of cells used was 1 million with a minimum size of 0.2 meter. CFD Ansys Fluent was used to simulate the urban microclimatic parameters in and around the area of interest. The first step of the simulation was to validate the results obtained from the
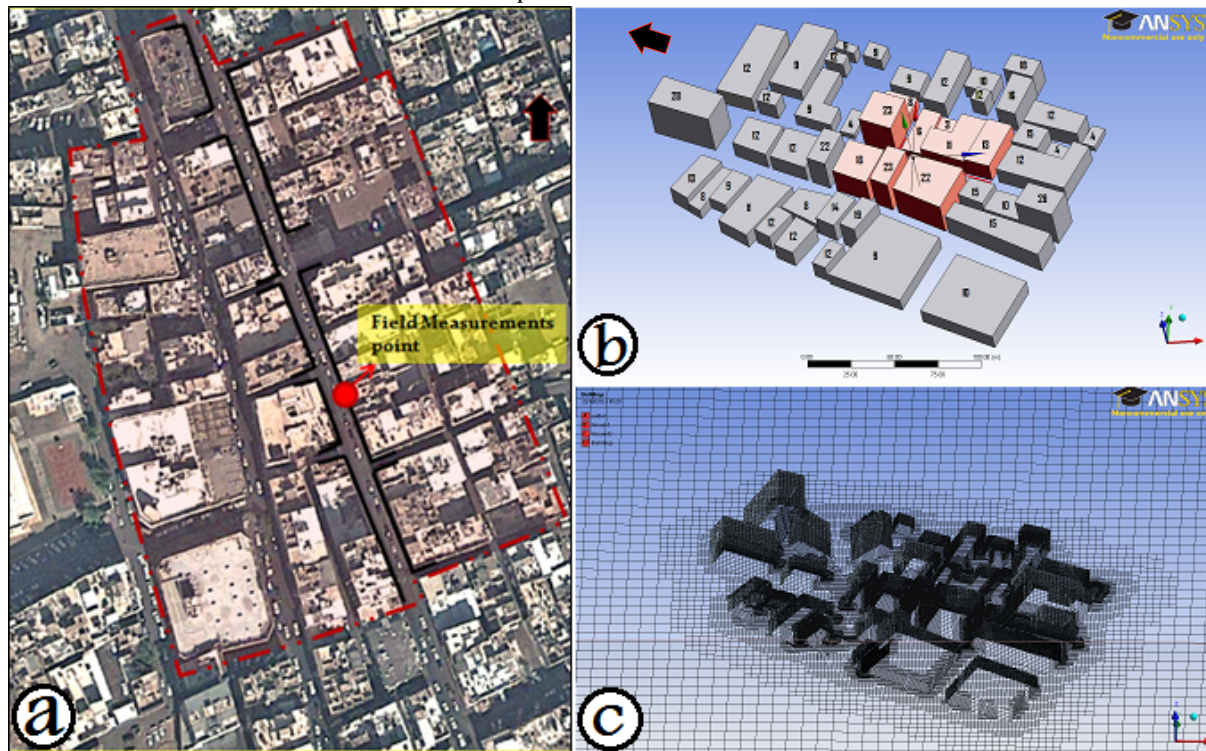

FIG. 8: a) Case study area of Quba Road, Madinah; b) 3D geometry; c) applying meshing on the geometry

CFD tool against the field measurements. Feedback from practice indicates that the acceptable error with the CFD results is up to 20% error (Wilkinson et al., 2013).

The CFD simulation was applied to the case study area using a steady RANS solver with realizable k-ε model and a standard wall function. This simulation was computed using a discrete ordinates (do) radiation model and energy model. A Second-order scheme was used with SIMPLE solver. A user defined function file was implemented in Ansys Fluent using the previously mentioned formulas for wind velocity profile U, the kinetic energy k, turbulence dissipation rate ε and friction velocity U^*, as given by Eqn. 6; 8; 9; and 10, respectively. The solution in FLUENT was considered to be converged when the convergence values dropped below 1e-04 and plot stopped varying and slope became zero (as shown in Fig.5 above). The validation of the results of the existing situation showed a good agreement between the data obtained from CFD simulation and the data obtained during field measurements as shown in Fig. 9 for the air temperature and in Fig. 10 for the air velocity. The boundary condition for the air temperature at the inlet was the specified heat flux temperature taking into account the radiation model. As a result the air temperature and air velocity were far below the acceptable maximum limit of errors (i.e. maximum of 20%). The air temperature in the simulation was resulted similar to the field measurement reading of 30°C at the measurement point. The air velocity was 6.5 m/s in the simulation and 7.0m/s in the field measurement, which both strongly validate the result of the CFD.

To enhance the thermal environment condition, the building arrangement with wind method was used in the modified version of the study. This approach was applied by increasing the height of the buildings that are located at the far ends of the road and in between. This has the effect of increasing the wind speed by forcing the wind at the top of the buildings towards the ground. A new street was also created in the direction of the prevailing wind (which is blowing from a south westerly direction). The results showed that this method decreases the air temperature by 2°C along several parts of the street (see Fig. 11). It also promotes wind movement along the road, increasing the wind speed by up to 1.3m/s above that measured before the building

layout was changed (see Fig. 12). Blocken et al. (2008) found that passages between two appropriately situated narrow perpendicular buildings can enhance the wind environmental conditions.
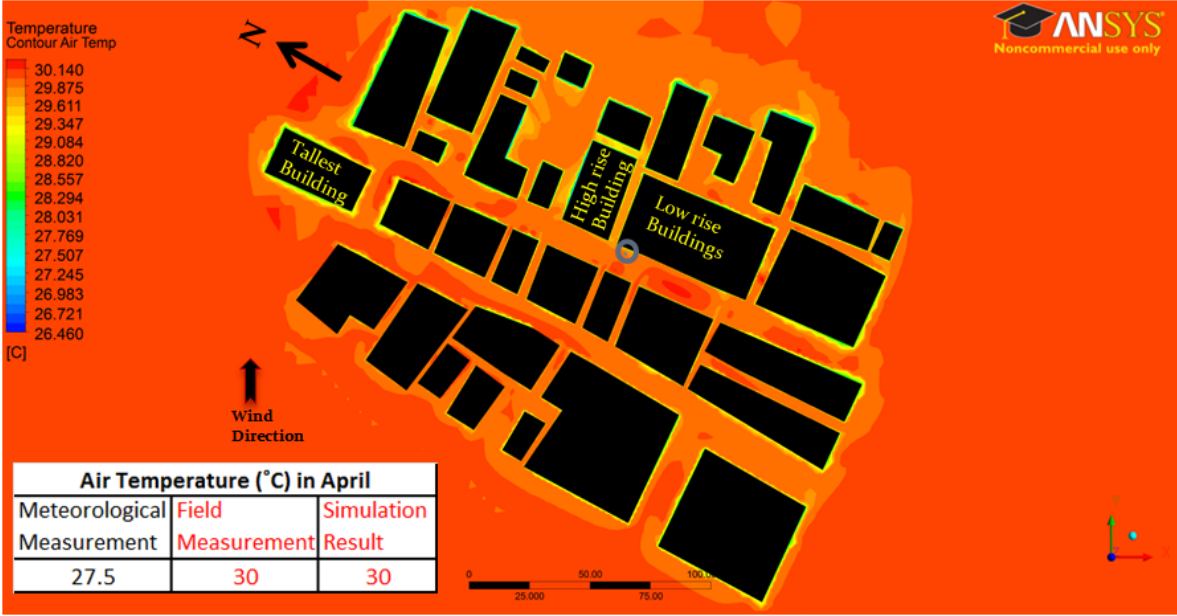

FIG. 9: Comparison of the air temperature data between the field measurement and the CFD result of the current situation. Note that the meteorological data is obtained from the airport, away from the urban area.
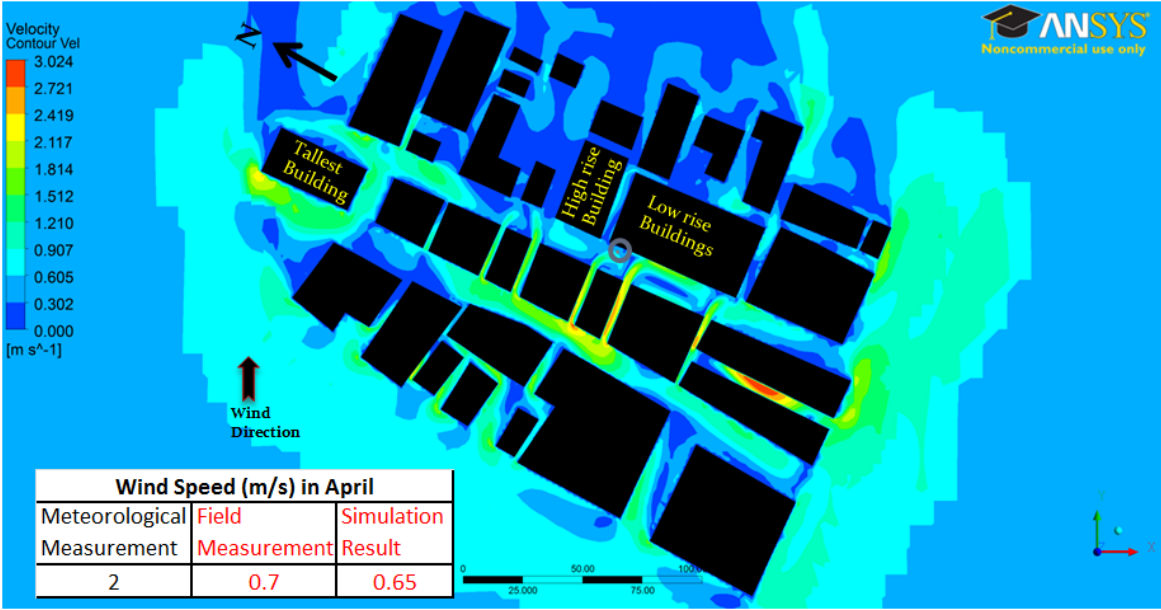

FIG. 10: Comparison of the air velocity data between the field measurement and the CFD result of the current situation. Note that the meteorological data from the suburban area is 1.3m/s higher than the urban area.

This method was also used in this study and validated its use as a method to increase wind movement and speed. The effects of changing the ground and building surface materials by pedestrianizing part of the street and the

use of appropriate color materials for buildings, as well as the introduction of water features and vegetation will form the topic of subsequent research efforts.
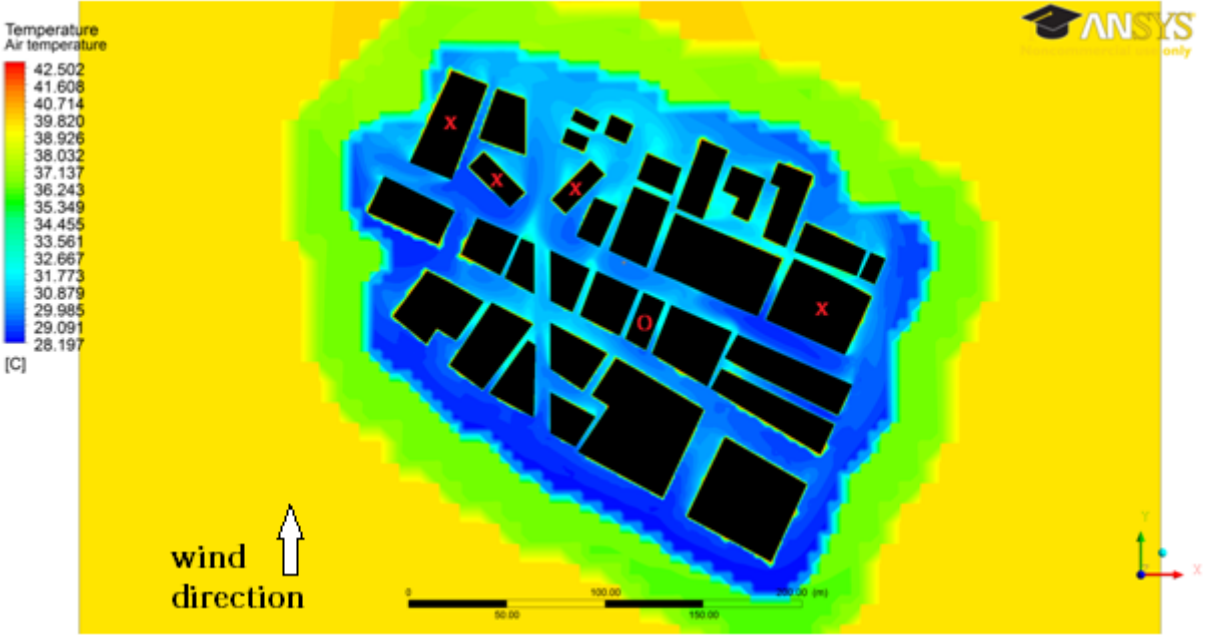

FIG. 11: Enhanced Air temperature by maximum of 2 degrees through implementing new high rise buildings (X) or extending the height of the existing building (X), and reducing the height in the centre (O).
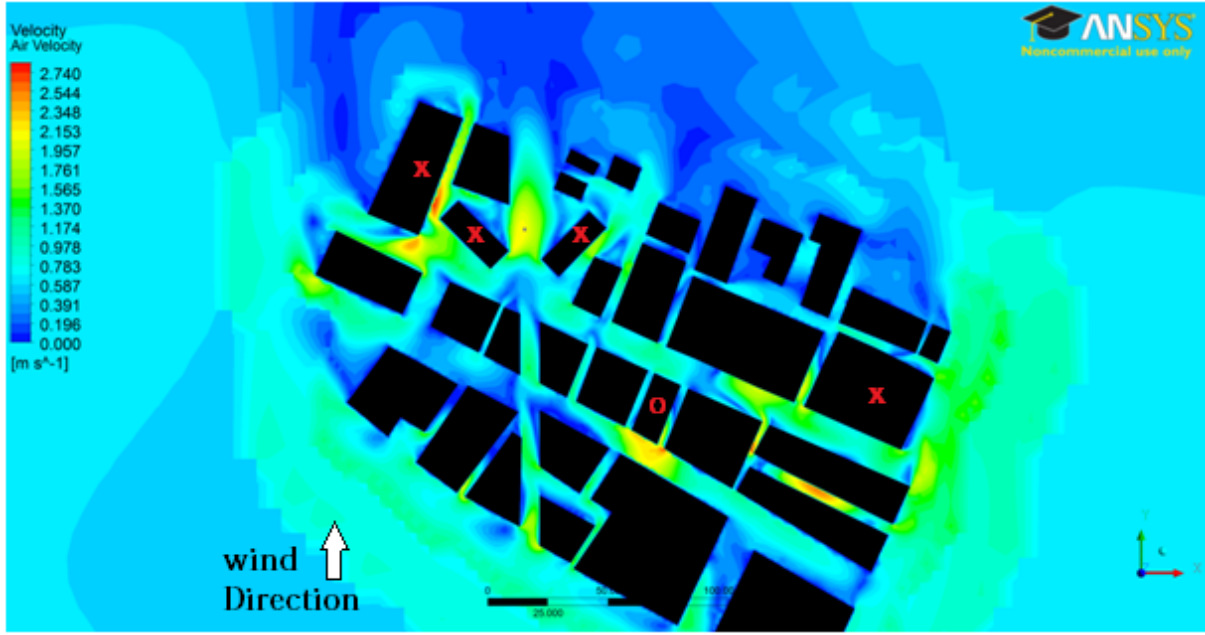

FIG. 12: Enhanced Air velocity by maximum of 1.3 to 2.3 m/s through implementing new high rise buildings (X) and introducing two 45° tall rectangular buildings along the proposed new road.

8. CONCLUSION

This paper discussed the potential of adopting the CFD simulation technique as a tool for the assessment of the complex fluid flows in urban thermal environments. A case study of an urban street was conducted using CFD to assess the outdoor pedestrian thermal comfort in hot dry climate of Madinah, Saudi Arabia. Three sites were selected for the assessment of thermal comfort (high density, medium density and low density areas). Only high density area was simulated with the aim of extending the possible use of outdoor space in non-peak summer conditions. By modifying the orientation of selected buildings and by creating a road in the direction of the wind, it was shown that this method increased the wind speed by forcing the wind at top of the buildings towards the ground, promoted wind movement along the road, and decreased the air temperature by $2^{o}C$ along several parts of the street. The increase in wind speed was up to 1.3m/s higher than the case before the modification in the urban geometry. The advantage of CFD is that it can be used to evaluate a range of issues comprising air speed and movement, air quality and pollution diffusion, wind comfort and thermal comfort as well as the effects of relative humidity and vegetation on indoor and outdoor spaces (Blocken and Persoon, 2009; Tominaga and Stathopoulos, 2009; Chung and Choo, 2011). There are three main steps for running CFD simulation, which starts with the creation of the building or system geometry, followed by grid generation using appropriate cell types (e.g. tetrahedral, pyramidal, prismatic and hexahedral cells), and then running mathematical solution of the problem via simulation. There are variant CFD solvers, such as LES, RANS, DES and DNS. The Reynolds Averaged Navier Stokes (RANS) approach is a modeling method in which the major variables such as temperature and velocity are divided into time-averaged and a turbulent fluctuation, and then turbulent model is used to model the turbulent fluctuation. RANS model is reasonably suitable for simulating wind flow in urban environment, and has increasingly been used for wind studies at pedestrian level. The advantages of RANS include its availability in all CFD codes, inexpensive and widely validated for urban studies. The paper has highlighted important guidelines from for the simulation of flows in urban environment and simulation of pedestrian wind comfort and thermal comfort.

9. REFERENCES

Abdel-Ghany, A.M., Al-Helal, I.M. and Shady, M.R. (2013) 'Human Thermal Comfort and Heat Stress in an Outdoor Urban Arid Environment: A Case Study', *Advances in Meteorology*, 2013, pp. 1-7.

Al-Ghamdi, M.S.H.A.-A. (1993) *Assessment and Improvement of Thermal Conditions inside Pilgrimage Tents at Makkah, Saudi Arabia*. University of Newcastle-upon-Tyne [Online].

This paper is available electronically at: https://theses.ncl.ac.uk/dspace/bitstream/10443/403/1/Al-Ghamdi93.pdf.

AUTODESK (2011). CFD workflow 4: solving and convergence. Autodesk sustainability workshop.

This paper is available electronically at http://sustainabilityworkshop.autodesk.com/products/cfd-workflow-4-solving-and-convergence, Accessed on 24th May 2013.

Barton, C. and Babister, M. (2012) *Australian Rainfall and Runoff - Revision Project 15: Two Dimensional Modelling in Urban and Rural Floodplains*. Institution of Engineers Australia. [Online].

This paper is available electronically at:
http://www.ncwe.org.au/arr/Website_links/ARR_Project15_TwoDimensional_Modelling_DraftReport.pdf

Bartzis, J.G., Vlachogiannis, D. and Sfetsos, A. (2004) 'Thematic Area 5: Best Practice Advice for Environmental Flows', *The QNET-CFD Network Newsletter*, 2(4), pp. 34-39.

Blocken B., Roels S. and Carmeliet J. (2004). Modification of Pedestrian Wind Comfort in the Silvertop Tower Passages by an Automatic Control System, *Journal of Wind Engineering and Industrial Aerodynamics*, 92(10), 849-873.

Blocken, B., Stathopoulos, T. and Carmeliet, J. (2007) 'CFD Simulation of the Atmospheric Boundary Layer: Wall Function Problems', *Atmospheric Environment*, 41(2), pp. 238-252.

Blocken B, Stathopoulos T, Carmeliet J. (2008). Wind environmental conditions in passages between two long narrow perpendicular buildings. *Journal of Aerospace Engineering –ASCE* 21(4): 280-287.

Blocken B. and Persoon J. (2009). Pedestrian wind comfort around a large football stadium in an urban environment: CFD simulation, validation and application of the new Dutch wind nuisance standard. *Journal of wind engineering and industrial aerodynamics,* 97 (5-6), 255-270.

Blocken B., Stathopoulos T., Carmeliet J. and Hensen J. (2009). Application of CFD in Building Performance Simulation for the Outdoor Environment, *11th International IBPSA Conference: Building Simulation.* Scotland: Glasgow, 27-30 July. 489-496.

Blocken B., Janssen W.D. and van Hooff T. (2012). CFD simulation for pedestrian wind comfort and wind safety in urban areas: General decision framework and case study for the Eindhoven University campus. Environmental Modelling & Software Vol. 30, 15-34

Catalano P. and Amato M. (2003). An evaluation of RANS turbulence modelling for aerodynamic applications. Aerospace science and technology, 7, 493–509

Chen Q. and Zhai Z. (2004). The use of CFD tools for indoor environmental design. Advanced Building Simulation, Edited by A. Malkawi and G. Augenbroe, Spon Press, New York, pp. 119-140.

Chung D. H. J. and Choo M.-L. L. (2011). Computational fluid dynamics for urban design: the prospects for greater integration. *International journal of architectural computing, 9***,** 33-54.

Cook M., Ji Y., and Gary Hunt G. (2005). CFD Modelling Of Buoyancy-Driven Natural Ventilation Opposed By Wind. Ninth International IBPSA Conference, Building Simulation, 2005, Montréal, Canada.

Coutts A.M., Beringer J. and Tapper N.J. (2007). Impact of Increasing Urban Density on Local Climate: Spatial and Temporal Variations in the Surface Energy Balance in Melbourne, Australia, *Journal of Applied Meteorology and Climatology*, 46(4), 477-493.

Durbin, P.A. and Pettersson Reif, B.A. (2001; 2011) *Statistical Theory and Modeling for Turbulent Flows*. 2nd edn. United Kingdom: John Wiley & Sons, Ltd.

Epstein J.M., Pankajakshan R. and Hammond R.A. (2011). Combining Computational Fluid Dynamics and Agent-Based Modeling: A New Approach to Evacuation Planning, *PLoS ONE*, 6(5), pp. 1-5.

Erell E., Pearlmutter D. and Williamson T. J. (2011). *Urban microclimate: designing the spaces between buildings,* London, Earthscan.

Fluent 6.3 (2006). *User's Guide*. Lebanon: Fluent Inc.

This paper is available electronically at: http://aerojet.engr.ucdavis.edu/fluenthelp/pdf/gs/flgs.pdf.

Franke J., Hirsch C., Jensen A.G., Krus H.W., Schatzmann M., Westbury P.S., Miles S.D., Wisse J.A. and Wright N.G. (2004). Recommendations on the Use of CFD in Wind Engineering, *In: van Beeck, J.P.A.J. (Ed.), COST Action C14, Impact of Wind and Storm on City Life Built Environment.* Proceedings of the International Conference on urban Wind Engineering and Building Aerodynamics, 5-7 May. von Karman Institute, Sint-Genesius-Rode, Belgium.

Franke J. (2006). Recommendations of the COST Action C14 on the Use of CFD in Predicting Pedestrian Wind Environment, *The Fourth International Symposium on Computational Wind Engineering (CWE2006)*. Japan: Yokohama. 529-532.

Franke J., Hellsten A., Schlunzen H. and Carissimo B. (2007). Best Practice Guideline for the CFD Simulation of Flows in the Urban Environment, *COST Action 732: Quality Assurance and Improvement of Microscale Meteorological Models*, 1-52.

Furbo E., Harju J. and Nilsson H. (2009). Evaluation of turbulence models for prediction of flow separation at a smooth surface. Report in scientific computing advanced course, Project 9.

Gousseau P., Blocken B., Stathopoulos T. and van Heijst G.J.F. (2011). CFD simulation of near-field pollutant dispersion on a high resolution grid: A case study by LES and RANS for a building group in downtown Montreal. Atmospheric Environment Vol. 45, 428-438

Harris, R.I. and Deaves, D.M. (1981) 'The Structure of Strong Winds', *Paper 4, CIRA Conference on Wind Engineering in the Eighties*. London. Construction Industry Research and Information Association.

He, J. and Song, C.C.S. (1999). Evaluation of Pedestrian Winds in Urban Area by Numerical Approach, *Journal of Wind Engineering and Industrial Aerodynamics*, 81(1–3), 295-309.

Hoppe P. (2002). Different Aspects of Assessing Indoor and Outdoor Thermal Comfort, *Elsevier Science Journal of Energy and Buildings*, 34, 661-665.

Isenstadt S. and Rizvi K. (2008). *Modernism and the Middle East: architecture and politics in the twentieth century,* U.S.A: Seattle, Library of congress cataloging-in-publication data.

Janssen W.D., Blocken B. and van Hooff T. (2013). Pedestrian Wind Comfort around Buildings: Comparison of Wind Comfort Criteria Based on Whole-Flow field Data for a Complex Case Study, *Journal of Building and Environment*, 59(0), pp. 547-562.

Li X., Koh T., Britter R., LIU C., Norford L. K., Entekhabi D. and Leung D. Y. C. (2009). Large-Eddy Simulation of flow field and pollutant dispersion in urban street canyons under unstable stratifications. The seventh international conference on urban climate, 29 June - 3 July 2009, Yokohama, Japan.

Lin T-P. (2009). Thermal perception, adaptation, and attendance in a public square in hot and humid regions. *Building and environment*, 44(10), 2017-2026

Masnavi M. R., Laghai H. and Ghobadi N. (2012). Eco design and the optimization of passive cooling ventilation for energy saving in the buildings: a framework for prediction of wind environment and natural ventilation in different neighborhood patterns. *Design for innovative value towards a sustainable society*, 177-182.

McAlpine J. D. and Ruby M. (2004). Using CFD to Study Air Quality in Urban Microenvironments. Chapter 1 of Environmental Sciences and Environmental Computing. Vol. II (P. Zannetti, Editor). Published by The EnviroComp Institute.

Meroney N. (2009). CFD Prediction of Airflow in Buildings for Natural Ventilation. 11th Americas Conference on Wind Engineering, June 22-26, 2009, San Juan, Puerto Rico

Mirzaei P.A. and Haghighat F. (2010). Approaches to study urban heat island – abilities and limitations. *Building and environment*, 45, 2192-2201

Mochida A., Tominaga Y., Murakami S., Yoshie R., Ishihara T. and Ooka R. (2002). Comparison of Various k–ε Models and DSM Applied to Flow Around a High-Rise Building: Report on AIJ Cooperative Project for CFD Prediction of Wind Environment, *Journal of Wind and Structures*, 5(2-4), pp. 227-244.

Mohammed M. A., Dudek S.J.M. and Hamza N. (2013). Simulation of Natural Ventilation in Hospitals of Semi-arid Climates for Harmattan Dust and Mosquitoes: A Conundrum. Proceedings of the 13th Conference of International Building Performance Simulation Association, August 26-28, Chambery, France.

Moonen P., Defraeye T., Dorer V., Blocken B. and Carmeliet J. (2012). Urban physics: effect of the micro-climate on comfort, health and energy demand, *Journal of frontiers of architectural research*, 1(3), 197-228.

Murakami S., Ooka R., Mochida A., Yoshida S. and Kim, S. (1999). CFD Analysis of Wind Climate from Human Scale to Urban Scale, *Journal of Wind Engineering and Industrial Aerodynamics*, 81(1–3), 57-81.

NAFMS (2013). General guidelines for good convergence in CFD.

This paper is available electronically at http://www.nafems.org/resources/cfdconvergence/Page0, Accessed on 24th May, 2013.

Nielsen (ed) P.V., Allard F., Awbi H.B., Davidson L. and Schälin A. (2007). *Computational Fluid Dynamics in Ventilation Design*. Brussels: REHVA Guide Book 10. RHEVA (Federation of European Heating and Air-Conditioning Association).

Poreh M. (1996). Investigation of heat islands using small scale models. *Atmospheric environment*, 30, 467–474

Priyadarsini, R., Hien, W.N. and Wai David, C.K. (2008) 'Microclimatic Modeling of the Urban Thermal Environment of Singapore to Mitigate Urban Heat Island', *Solar Energy*, 82(8), pp. 727-745.

Ramponi R. and Blocken B. (2012). CFD simulation of Cross-Ventilation for a Generic Isolated Building: Impact of Computational Parameters, *Building and Environment*, 53(0), 34-48.

Richards, P.J. (1989) *Computational Modelling of Wind Flows around Low Rise Buildings Using PHOENIX*. Report for the ARFC Institute of Engineering Research Wrest Park, Silsoe Research Institute, UK: Bedfordshire.

Richards, P.J. and Hoxey, R.P. (1993) 'Appropriate Boundary Conditions for Computational Wind Engineering Models Using the k-ϵ Turbulence Model', *Journal of Wind Engineering and Industrial Aerodynamics*, 46–47(0), pp. 145-153.

Santiago J.L., Dejoan A., Martilli A., Martin F. and Pinelli A. (2010). Comparison between Large-Eddy Simulation and Reynolds-Averaged Navier-Stokes Computations for the MUST Field Experiment. Part I: Study of the Flow for an Incident Wind Directed Perpendicularly to the Front Array of Containers, *Boundary-Layer Meteorology*, 135(1), 109-132.

Sengupta K. and Mashayek F. (2008). Direct numerical simulation of turbulent flows using spectral methods, 46th AIAA Aerospace sciences meeting and exhibition 7 - 10 January 2008, Reno, Nevada.

Setaih, K., Hamza, N. and Townshend, T. (2013) 'Use of CFD Simulation in Urban Design for Outdoor Thermal Comfort in Hot and Dry Climates: A Review', *International PostGraduate Research Conference (IPGRC)*, 8-10 of April. pp. 1069-1076.

This paper is available electronically at
http://www.researchgate.net/publication/236259428_Performance_improvement_in_Public_Sector_Framework_Agreements.

Setaih, K., Hamza, N. and Townshend, T. (2013) 'Assessment of Outdoor Thermal Comfort in Urban Microclimate in Hot Arid Areas', *Proceedings of BS2013: 13th Conference of International Building Performance Simulation Association*. Chambéry, France, 26-28 of August. pp. 3153-3160.

This paper is available electronically at: http://www.ibpsa.org/proceedings/BS2013/p_2521.pdf

Shirasawa T., Tominaga T., Yohshie R., Mochida A., Yoshino H., Kataoka H. and Nozu T. (2003). Development of CFD Method for Predicting Wind Environment around a High-Rise Building - Part 2: the Cross Comparison of CFD results using Various k– Models for the Flowfield around a Building Model with 4:4:1 Shape, *AIJ Journal of Technology and Design*, 18, pp. 169-174 *(in Japanese)*.

Spalart R. (2009). Detached-Eddy Simulation annual reviews of fluid mechanics, 41:181–202.

Stavrakakis G.M., Tzanaki E., Genetzaki V.I., Anagnostakis G., Galetakis G. and Grigorakis E. (2012). A Computational Methodology for Effective Bioclimatic-Design Applications in the Urban Environment, *Sustainable Cities and Society*, 4(0), 41-57.

Taleb, H. and Taleb, D. (2014) 'Enhancing the Thermal Comfort on Urban Level in a Desert Area: Case study of Dubai, United Arab Emirates', *Urban Forestry & Urban Greening*, (0).

This paper is available electronically at: http://http://www.sciencedirect.com/science/article/pii/S1618866714000077

Tan S.-A. and Fwa T.-F. (1992). Influence of Pavement Materials on the Thermal Environment of Outdoor Spaces, *Building and Environment*, 27(3), 289-295.

Tominaga, Y., Yoshie, R., Mochida, A., Kataoka, H., Harimoto, K. and Nozu, T. (2005) 'Cross Comparisons of CFD Prediction for Wind Environment at Pedestrian Level around Buildings - Part 2: Comparison of Results for Flowfield around Building Complex in Actual Urban Area', *The Sixth Asia-Pacific Conference on Wind Engineering (APCWE-VI)*. Korea: Seoul, 12-14 September. pp. 2661-2670.

Tominaga Y., Mochida A., Murakami S. and Sawaki S. (2008). Comparison of various revised k-e models and LES applied to flow around a high-rise building model with 1:1:2 shape placed within the surface boundary layer. *Journal of wind engineering and industrial aerodynamics,* 96**,** 389-411.

Tominaga Y., Mochida A., Youshie R., Kataoka H., Nozu T., et al. AIJ (2008). Guidelines for Practical Applications of CFD to Pedestrian Wind Environment around Buildings. Journal of Wind Engineering & Industrial Aerodynamics. 96, 1749-61

Tominaga Y. and Stathopoulos T. (2009). Numerical simulation of dispersion around an isolated cubic building: comparison of various types of k-ε models. *Journal of atmospheric environment,* 43(20*), 3200-3210.

Uddin N. (2008). Turbulence modeling of complex flows in CFD. A thesis accepted by the Faculty of Aerospace Engineering and Geodesy of the Universität Stuttgart in partial fulfillment of the requirements for the degree of Doctor of Engineering Sciences.

van Hooff, T. and Blocken, B. (2010) 'Coupled urban wind flow and indoor natural ventilation modelling on a high-resolution grid: A case study for the Amsterdam ArenA stadium', *Environmental Modelling & Software*, 25(1), pp. 51-65.

Van Hooff T. and Blocken B. (2013). CFD evaluation of natural ventilation of indoor environments by the concentration decay method: CO2 gas dispersion from a semi-enclosed stadium. Building and Environment Vol. 61, 1-17.

Voogt A. and Oke T.R. (2003). Thermal remote sensing of urban climates. *Remote sensing of environment*, 86, 370–384.

Walton A., Cheng A.Y.S. and Yeung W.C. (2002). Large-eddy Simulation of Pollution Dispersion in an Urban Street Canyon—Part I: Comparison with Field Data, *Atmospheric Environment*, 36(22), 3601-3613.

Wieringa, J. (1992) 'Updating the Davenport Roughness Classification', *Journal of Wind Engineering and Industrial Aerodynamics*, 41(1–3), pp. 357-368.

Wilkinson S., Hanna S., Hesselgren L., and Mueller V. (2013). Inductive Aerodynamics. Stouffs, Rudi and Sariyildz, Sevil (eds.), Computation and Performance, Proceedings of the 31st eCAADe Conference, vol 2. The Netherlands, 18-20 September 2013, 29-48.

Yang T. (2004). CFD and Field Testing of a Naturally Ventilated Full-scale Building. PhD thesis. University of Nottingham.

Yoshie, R., Mochida, A., Tominaga, Y., Kataoka, H. and Yoshikawa, M. (2006) 'CFD Prediction of Wind Environment around a High-rise Building Located in an Urban Area', *The Fourth International Symposium on Computational Wind Engineering (CWE2006)*. Japan: Yokohama. pp. 129-132.

Yoshie R., Mochida A., Tominaga Y., Kataoka H., Harimoto K., Nozu T., Shirasawa T. (2007). Cooperative Project for CFD Prediction of Pedestrian Wind Environment in the Architectural Institute of Japan, *Journal of Wind Engineering and Industrial Aerodynamics,* 95(9-11):1551-1578.

Zoumakis, N.M. and Kelessis, A.G. (1991) 'Methodology for Bulk Approximation of the Wind Profile Power-Law Exponent under Stable Stratification', *Boundary-Layer Meteorology*, 55(1-2), pp. 199-203.